

Particle renormalizations in presence of dissipative environments

Victor Kagalovsky¹ and Baruch Horovitz²

¹ Sami Shamoon College of Engineering, Beer-Sheva, 84100 Israel and

² Department of Physics, Ben Gurion university, Beer Sheva 84105 Israel

We study the Aharonov-Bohm oscillations of a charged particle on a ring of radius R coupled to a dirty metal environment. With Monte-Carlo methods we evaluate the curvature of these oscillations which has the form $1/M^*R^2$, where M^* is an effective mass. We find that at low temperatures T the curvature approaches at large $R > l$ an R independent $M^* > M$, where l is the mean free path in the metal. This behavior is also consistent with perturbation theory in the particle - metal coupling parameter. At finite temperature T we identify dephasing lengths that scale as T^{-1} at $R \gtrsim l$ and as $T^{-1/4}$ at $R \ll l$.

PACS numbers: 73.43.Nq, 73.23.Ra, 74.40.+k

I. INTRODUCTION

The problem of interference in presence of a dissipative environment is fundamental for a variety of experimental systems. Interference has been monitored by Aharonov-Bohm (AB) oscillations in mesoscopic rings^{1,2,3} or in quantum Hall edge states⁴ in presence of noise from gates or other metal surfaces. Cold atoms trapped by an atom chip are sensitive to the noise produced by the chip^{5,6,7}. In particular giant Rydberg atoms are studied⁸ whose huge electric dipole is highly susceptible to such noise.

An efficient tool for monitoring the effect of the environment, as proposed by Guinea⁹, is to find the AB oscillation amplitude as function of the radius R of the ring. This amplitude is measured by the curvature^{10,11,12} of the ground state energy E_0 at external flux $\phi_x = 0$, i.e. $1/M^*R^2 = \partial^2 E_0 / \partial \phi_x^2|_0$, defining an effective mass M^* . For free particles of mass M this curvature is the mean level spacing $1/MR^2$. The particle can be coupled to a variety of environments, with three systems of particular interest: (i) a Caldeira-Legget (CL) bath⁹, (ii) a charged particle in a dirty metal environment^{9,13} and (iii) a particle with an electric dipole in a dirty metal environment¹⁴. System (i) has been studied with a large variety of methods, all showing that the AB amplitude is exponentially suppressed $\sim e^{-\pi^2 \gamma R^2}$, i.e. a new length scale $\sim 1/\sqrt{\gamma}$ is generated by the coupling γ to the environment⁹. System (ii) has been studied by renormalization group (RG) methods^{9,15} finding $M^* \sim R^\mu$ with a small μ , a Monte Carlo (MC) numerical method gave¹³ $\mu = 1.8$ at sufficiently large R , while a variational scheme¹⁴ gave $\mu = 0$. System (iii) was also studied within the variational scheme¹⁴, leading to $\mu = 0$ as well.

In the present work we use MC methods to analyze mostly system (ii). We find that the energy cutoff used in a previous study¹³ is insufficient and a higher cutoff ω_c is needed. In particular we find that at large $R > l$ the effective mass M^* is R independent, i.e. $\mu = 0$, where l is the mean free path in the metal. For $R > l$ we also find that at temperature T the data scales as TR , identifying a length scale $\sim 1/T$. For $R \ll l$ the system reduces to a CL one with a $\sim T^{-1/4}$ length scale.

A non-equilibrium study¹⁶ has found dephasing lengths that have the same power laws, establishing a connection between equilibrium and non-equilibrium results.

II. THE MODEL

The time dependent angular position $\theta_m(\tau)$ of a particle on the ring has in general a winding number m so that $\theta_m(\tau) = \theta(\tau) + 2\pi m T \tau$ where $\theta(0) = \theta(1/T)$ has periodic boundary condition. In presence of an external flux ϕ_x (in units of the flux quantum hc/e) the partition sum has the form

$$Z = \sum_m e^{2\pi i m \phi_x} \int \mathcal{D}\theta e^{-S^{(m)}}$$

$$S^{(m)} = \frac{1}{2} M R^2 \int_0^{1/T} \left(\frac{\partial \theta}{\partial \tau} + 2\pi m T \right)^2 d\tau +$$

$$\alpha \int_0^{1/T} \int_0^{1/T} \frac{\pi^2 T^2 K[\theta(\tau) - \theta(\tau') + 2\pi m T(\tau - \tau')]}{\sin^2 \pi T(\tau - \tau')} d\tau d\tau' \quad (1)$$

where the effect of environments, in each of the 3 cases, is^{9,13,14}

$$K(z) = \begin{aligned} & \sin^2 z/2; & \alpha &= \gamma R^2 & (i) \\ & = 1 - [4r^2 \sin^2 \frac{z}{2} + 1]^{-1/2}; & \alpha &= \frac{3}{8k_F^2 l^2} & (ii) \\ & = 1 - [4r^2 \sin^2 \frac{z}{2} + 1]^{-3/2}; & \alpha &= \frac{p^2}{e^2 l^2} \frac{3}{8k_F^2 l^2} & (iii). \end{aligned} \quad (2)$$

Case (i) is the CL system where γ is the coupling to a harmonic oscillator bath; case (ii) is a charge coupled to a dirty metal where k_F is the Fermi wavevector, l is the mean free path in the metal, and $r = R/l$; case (iii) is an electric dipole of strength p coupled to a dirty metal.

We note that the forms (ii) and (iii) are based^{13,14} on a wavevector and frequency dependent dielectric function for the metal of the form $\epsilon(q, \omega) = 1 + 4\pi\sigma/(-i\omega + Dq^2)$ valid at $q < 1/l$, where σ is the conductivity and D is the diffusion constant of the metal. The q integrals are cutoff

by $q < 1/\ell$, hence the the forms (ii) and (iii) are valid at $r \gtrsim 1$. We will use below these forms also at $r < 1$ since they represent qualitatively the decrease of $K(z)$ with r . Furthermore, at $r \rightarrow 0$ the form (ii) reduces to that of the CL model (i) with $\alpha_{CL} = 2\alpha r^2$.

We also note that in model (ii) $\alpha < 1$ for relevant metals. However, model (iii) allows for a large α since the dipole parameter p can be large, as e.g. in the Rydberg atoms⁸.

We are interested in the effect of the environment on the visibility of quantum interference as measured by the particle. As a measure of this visibility we consider the curvature of the Aharonov-Bohm oscillations

$$\frac{1}{M^*(T)R^2} = \frac{\partial^2 F}{\partial \phi_x^2} \Big|_{\phi_x=0} \quad (3)$$

where $F = -T \ln Z$. It is useful to consider a free particle $\alpha = 0$, for which

$$\left(\frac{M}{M^*(T)} \right)_{\alpha=0} = 2\pi^2 t \sum_m m^2 e^{-\pi^2 m^2 t} / \sum_m e^{-\pi^2 m^2 t} \equiv f(t) \quad (4)$$

where $t = 2MR^2T$. This identifies the thermal length $L_T \sim 1/\sqrt{MT}$.

In the interacting system a high energy cutoff can be identified by considering $\tau \rightarrow \tau'$ (corresponding to high frequencies ω) so that expansion of $K(z)$ and Fourier transform yield

$$S^{(m)} \rightarrow \frac{1}{2} \int \frac{d\omega}{2\pi} [MR^2\omega^2 + 2\pi\alpha K''(0)|\omega|] |\theta(\omega)|^2 + (2\pi m)^2 [\frac{1}{2}MR^2T + \alpha K''(0)]. \quad (5)$$

The term linear in $|\omega|$ is typical for dissipative systems, i.e. the environment induces dissipation on the particle. The cutoff ω_c is now identified when the kinetic $\sim \omega^2$ and $\sim |\omega|$ interaction terms are comparable, i.e.

$$\omega_c = \frac{2\pi\alpha K''(0)}{MR^2}. \quad (6)$$

This ω_c replaces a possibly higher environment cutoff, since significant renormalizations start only below ω_c where the linear $|\omega|$ dispersion leads to $\ln \omega$ terms in perturbation theory and to the need for either RG treatment, or an equivalent variational scheme¹⁴. Note that $K''(0) = \frac{1}{2}; r^2; 3r^2$ in the 3 models above, hence $\omega_c = \pi\gamma/M$ in case (i), while $\omega_c \sim \alpha/Ml^2$ in cases (ii) and (iii).

III. MONTE CARLO PROCEDURE

For the MC numerical method we need to discretize the time axis into a Trotter number N_T of segments, i.e. the time interval of each segment is $\Delta\tau = 1/(TN_T)$. The discrete action is

$$S^{(m)} = \frac{1}{2} [MR^2 N_T T + \alpha K''(0)] \sum_n (\theta_{n+1} - \theta_n + \frac{2\pi m}{N_T})^2$$

$$+ \frac{\alpha\pi^2}{N_T^2} \sum_{n \neq n'} \frac{K(\theta_n - \theta_{n'} + 2\pi m(n - n')/N_T)}{\sin^2(\pi(n - n')/N_T)}. \quad (7)$$

The $\frac{1}{2}\alpha K''(0)$ term comes from the $n = n'$ interaction term by expanding $K(z)$ around $z = 0$. A key issue in our MC study is the choice of energy cutoff $1/\Delta\tau$ and the corresponding Trotter number $N_T = 1/(T\Delta\tau)$. The correct choice is such that the free kinetic term dominates over the single $n = n'$ interaction term, i.e. $N_T \gtrsim \omega_c/T$, with ω_c from Eq. (6). Hence $\Delta\tau \approx 1/\omega_c$ corresponds to the cutoff ω_c as identified by RG or variational methods. A previous MC study on the charge problem¹³ has chosen N_T in the range $1/t$ to $4/t$, i.e. an energy cutoff of $\approx 1/MR^2$. For large r this cutoff is much smaller than ω_c and is therefore insufficient.

Eqs. (1,3) identify $1/M^*(T)R^2 = 2\pi^2 T \langle m^2 \rangle \Big|_{\phi_x=0}$ so that the MC evaluates the fluctuations in winding number $\langle m^2 \rangle$ at external flux $\phi_x = 0$. The procedure is to start with some m , update θ_n at a time position n to θ'_n and accept or reject the change according to the MC rule with probability $\exp[S^{(m)}\{\theta_n\} - S^{(m)}\{\theta'_n\}]$. After the N_T points are successively updated, the winding number is shifted to $m' = m \pm 1$ and the shift is accepted or rejected with the probability $\exp[S^{(m')}\{\theta_n\} - S^{(m)}\{\theta_n\}]$. An update of θ_n is done randomly with a step size that produces an acceptance ratio of about 50%¹¹.

The inset in Fig. 1 shows the N_T dependence of M/M^* for the charge problem with $r = 5, t = 0.2, \alpha = 0.019$. A choice for N_T in the range $1/t - 4/t$ is clearly insufficient; saturation sets in around $N_T \approx 100$ which is of order of $\omega_c/T = 30$. In the following we choose our N_T , in the charge problem, to be $N_T = 40\alpha r^2/t = 10\omega_c/(\pi T)$, i.e. $N_T = 95$ for the inset parameters. For the dipole case, where ω_c is 3 times higher we choose $N_T = 120\alpha r^2/t = 10\omega_c/(\pi T)$. Fig. 1 shows that for $r = 5, t = 0.2, \alpha = 0.02$ (red squares) saturation indeed sets in near $N_T = 300$.

This high value of N_T restricts realistic MC studies. We have noticed, however, that this high N_T is necessary only in the vicinity of $n = n'$ in the double sum of (7), where the summand is rapidly varying. Hence the double sum is taken over all points only in the vicinity of the singularity, i.e. for $|n - n'| < 0.03N_T$. For points that are further separated we coarse grain the sum with fewer points, corresponding to an effective $N_T = 1/t$.

The results of this procedure are shown by the green circles in Fig. 1, and are in agreement with the full calculation that includes all N_T points. The double sum has then $\approx \frac{1}{2}10^{-3}N_T^2 + \frac{1}{2}t^{-2}$ terms, much less than the $\frac{1}{2}N_T^2$ terms of the full calculation. We also show data where the double sum is coarse grained at all points, including those near $n = n'$, by blue triangles. Here the double sum has only $\frac{1}{2}t^{-2}$ terms; this data has significant deviations from the full calculation.

We proceed to discuss our error estimates. At low temperatures we evaluate $\langle m^2 \rangle$, and the average involves typically many values of m . To estimate errors we evaluate the correlation function for a given run and deduce a correlation length ξ . We discard the initial 10^4 MC iter-

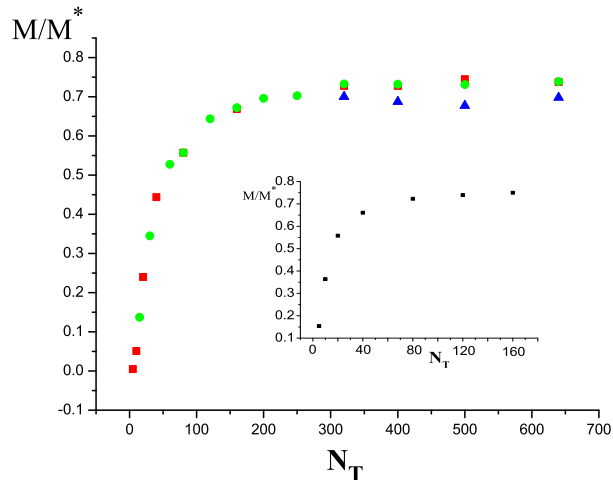


FIG. 1: Trotter number dependence of the effective mass for the dipole case with $r = 5, t = 0.2, \alpha = 0.02$, using (i) all N_T points in the double sum Eq. (7) – red squares, (ii) For points $|n - n'| > 0.03N_T$ sum is coarse grained (see text) – green circles, (iii) the whole sum is coarse grained – blue triangles. Inset: The charge case with $r = 5, t = 0.2, \alpha = 0.019$ using all N_T points in the sums.

ations and then evaluate the standard deviation σ of the average data; the error is then¹⁷ $\sigma\sqrt{2\xi + 1}$. We typically find a short correlation length of a few units and we run till an error of $\sim 2\%$ is achieved; the number of iterations is then $\approx (1 - 2) \cdot 10^5$ and in some cases up to 10^6 , where each iteration is an update of N_T values of the θ_n .

At high temperatures $t > 1$, where $M/M^* \lesssim 10^{-3}$, the probability of $m \neq 0$ becomes extremely small so that just $m = \pm 1$ determine the outcome¹¹. Hence we evaluate $\langle m^2 \rangle = 2\langle e^{S_1 - S_0} \rangle_0$, averaging with e^{-S_0} . In this method we find a rather long correlation length of $\sim 10^3$, yet there is no need to vary m and a 2% accuracy can be achieved after $\approx (1 - 2) \cdot 10^5$ iterations.

IV. MC RESULTS

We present here our data for the dirty metal, system (ii). In Fig. 2 we show our data for $\alpha = 0.019$ at low temperatures, $t < 0.3$; we note saturation at $t < 0.2$. In Fig. 3 we collect the limiting low t values of our data for various alpha, typically achieved at $t \approx 0.1 - 0.01$. The data is limited to Trotter numbers $N_T = 40\alpha r^2/t < 9000$.

We compare in Fig. 3 the data with results of perturbation theory (Appendix I). The perturbation is formally first order in α , however, it should be valid also for large α and small r such that $x \lesssim 2$, where at $t = 0$ we define $x = M^*(t = 0)/M$. The perturbation curves are a good fit to the data for $r \lesssim 1$, while at $r > 1$ and small α the

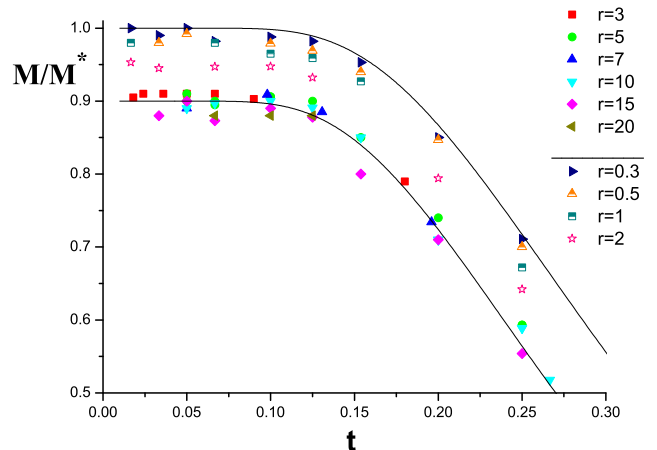


FIG. 2: AB curvature as function of reduced temperature with $\alpha = 0.019$. All $r \geq 3$ values fit the renormalized form $0.9f(t/0.9)$ – the lower curve. At $r \leq 1$ the data approaches $f(t)$ of a free particles – the upper curve.

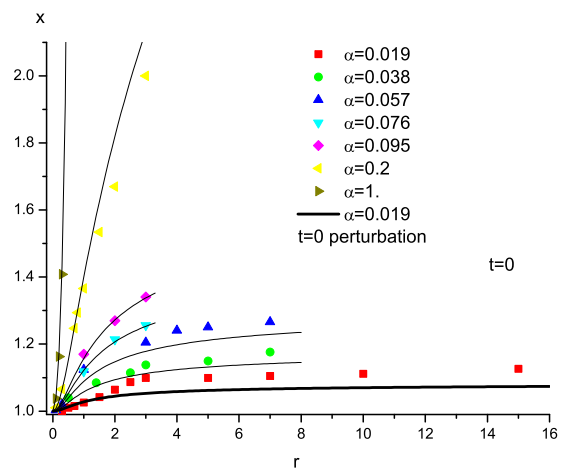


FIG. 3: $t = 0$ limiting values of $x = M^*(t = 0)/M$ for various α . The full lines are results of perturbation expansion (Appendix I).

fit is qualitatively good, in the sense that saturation is achieved at large r . We have also attempted to fit these data by a scaling function of the form $x = 1 + r^{2-c}g(\alpha r^c)$, that is consistent with the $r \rightarrow 0$ form of the perturbation expansion. In particular, this form with $c = 2$ would scale onto the CL system at $r \rightarrow 0, \alpha \rightarrow \infty$. However, we could not find a satisfactory fit even for the small $r \lesssim 2$ regime.

Our data shows for the lowest $\alpha = 0.019$ and for $r \geq 3$

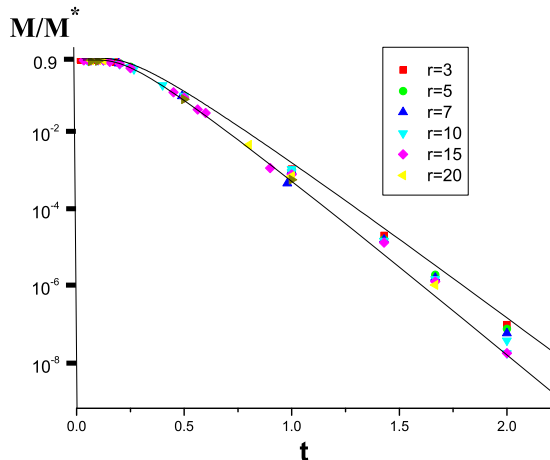


FIG. 4: AB curvature including high temperatures with $\alpha = 0.019$. All data fall in between the upper line $f(t)$ and the lower line $0.9f(t/0.9)$.

that M/M^* reaches saturation with $M/M^* \approx 0.9$, almost independent of r . The data at $r = 20$ (shown in Fig. 2) is consistent with this saturation, though it is not shown in Fig. 3 to keep a convenient scale. In view of this saturation at $3 < r < 20$ we expect it to persist at higher r . In terms of $M^* \sim r^\mu$, our data shows that $\mu \lesssim 0.05$ and is consistent with $\mu = 0$. We note that with our revised values of N_T we were not able to reach a saturation regime at larger α , see Fig. 3.

Our result shows that the AB curvature $\sim 1/R^2$ is the same as for free particles, i.e. the ground state has no anomaly, at least for weak $\alpha = 0.019$. Furthermore, Fig. 2 shows that M^* determines the finite temperature behavior, as long as $T \ll \omega_c$. Thus if we replace $M \rightarrow M^* = M/0.9$ in Eq. (4) we obtain the lower curve $0.9f(t/0.9)$ in Fig. 2 which is a good fit to the data. The thermal length is then $L_T \sim 1/\sqrt{M^*T}$.

In Fig. 4 we show our $r \geq 3$ data up to $t = 2$. The data falls in between two lines: $0.9f(t/0.9)$ and $f(t)$. The lower curve $0.9f(t/0.9)$ corresponds to the renormalized system and fits data with $T \ll \omega_c$, i.e. $t \ll 4\pi\alpha r^2$. For a fixed t as r decreases T approaches ω_c and the data approaches the upper curve which is the unrenormalized free particle form $f(t)$.

We therefore parameterize our data by a function $x(r, t)$ such that $M/M^* = f(tx)/x$. In this way we avoid the obvious t dependence associated with mass renormalization and focus on additional temperature effects. In Fig. 5 we show that for $r \gtrsim 1$ the data for $x(t, r)$ scales with t/r . Since $t \sim TR^2$ the scaling parameter is $\sim TR$, identifying a length scale $\sim 1/T$. A dephasing length scale has been recently derived in a non-equilibrium study¹⁶ which for $r \gtrsim 1$ indeed scales with $1/T$. We propose therefore that the additional T de-

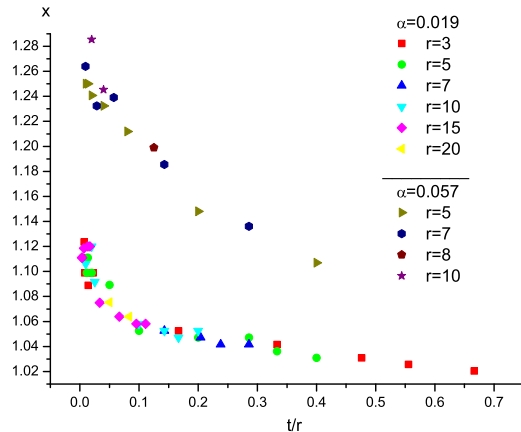


FIG. 5: Scaling of the x variable in $M/M^* = f(tx)/x$ for $r \gtrsim 1$ cases, with $\alpha = 0.019$ and $\alpha = 0.057$.

pendence embedded in our variable $x(t, r)$ is related to dephasing of the non-equilibrium situation.

We note that the perturbation expansion yields for $r \gg 1$,

$$\frac{M}{M^*} = 1 - 4\alpha + O\left(\frac{\alpha t}{r} \ln r\right) \quad r \gg 1. \quad (8)$$

While the dependence on t/r is consistent with Fig. 5 (up to a $\ln r$ factor), we note that the t/r form in the perturbation form (8) is valid only at $t \ll 1$ and $r \gtrsim 10$. Hence the observed scaling, Fig. 5, with t/r up to $t \approx 1$ and at $3 < r < 20$ is an unexpected feature.

In Fig. 6 we show that for $r \ll 1$ the data scales as tr^2 . At $tr^2 \lesssim 0.04$ both $x(t, r)$ and $x(0, r)$ are close to 1 and the errors in $1/x(t, r) - 1/x(0, r)$ are too large to draw a conclusion in this regime. The same difficulty is with all data of small α , hence Fig. 6 shows only $\alpha = 0.2, 1$. At $tr^2 \gtrsim 0.04$ the data in Fig. 6 supports a tr^2 scaling. Since $t \sim TR^2$ this implies a length scale $\sim T^{-1/4}$. We note again that similar dependence for a dephasing length was found for $r \ll 1$ in the non-equilibrium study¹⁶.

For $r \ll 1$ we can use the perturbation result Eq. (A12)

$$\frac{M}{M^*} = 1 - 2\alpha \sum_n a_n + 4tar^2 \quad r \ll 1. \quad (9)$$

This shows the αr^2 scaling at $tar^2 \ll 1$. It is remarkable that our data in Fig. 6 supports αr^2 scaling up to rather high temperatures of $t \lesssim 1$.

As noted above, the r dependence of $K(z)$ is reliable only at $r \gtrsim 1$ where the low q, ω form of $\epsilon(q, \omega)$ can be used, or at $r \ll 1$, which is the CL limit. In fact, for a general $\epsilon(q, \omega)$ one can expand the response in R and obtain that the leading term is $K(z) \sim R^2$, i.e. the CL form. We conclude then that at both small and large r ,

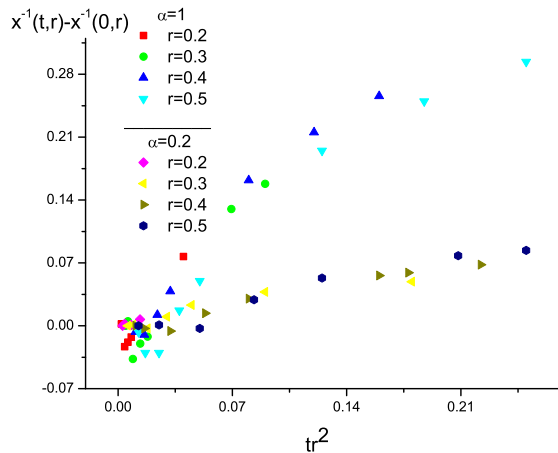


FIG. 6: Scaling of the variable $\frac{1}{x(t,r)} - \frac{1}{x(0,r)}$ for $r \ll 1$ cases, with $\alpha = 0.2$ and $\alpha = 1$.

where $K(z)$ is reliable, the T dependent length scale of the equilibrium observable M^*/M can be identified with a dephasing length.

V. DISCUSSION

The possible dependence of $M^*(r)$ at $T = 0$ has been of interest as a means of monitoring anomalies in the

ground state^{9,13} of metals. Previous studies proposed $M^* \sim r^\mu$ with either^{9,15} a small μ or¹³ $\mu = 1.8$ or¹⁴ $\mu = 0$. Instanton based arguments suggested¹³ a $M^*(r)$ dependence for $\alpha r > 1$.

With our revised values of N_T we were able to reach a reasonably large r only for weak coupling, $\alpha = 0.019$. For this coupling we observe saturation at $3 < r < 20$. Although we cannot strictly rule out $\mu \neq 0$ at higher r , we find it highly unlikely that an r dependence will reappear at $r > 20$. We propose then $\mu = 0$ at $\alpha = 0.019$, implying $\mu = 0$ at all α (if larger α would show a $\mu \neq 0$ it would imply an unlikely singular line in the α, r plane). We propose then that $\mu = 0$ for all α at $r \gg 1$ and that the effect of the environment is a mass renormalization, in agreement with the variational study¹⁴.

We have found temperature dependent length scales. For $r \gtrsim 1$ we find T^{-1} , while for $r \ll 1$ we find $T^{-1/4}$. We note that the same T dependence was found for dephasing lengths in a nonequilibrium study based on the purity of a reduced density matrix¹⁶ for the dirty metal situation. A dephasing length was deduced¹⁶ by comparing a dephasing rate with a mean level separation as a condition for coherence. It is remarkable that the agreement in these dephasing lengths is obtained in both regimes $r \gtrsim 1$ and $r \ll 1$ where the form of Eq. (2 ii) is valid for a dirty metal environment; the $r \ll 1$ form is also valid for other realizations of a CL environment. We have therefore the intriguing observation that equilibrium scales can identify non-equilibrium dephasing length scales.

APPENDIX A: PERTURBATION EXPANSION

Consider the action of a particle on a ring in presence of a dissipative environment and a flux ϕ_x through the ring Eq. (1) with the dirty metal environment:

$$K(z) = 1 - [4r^2 \sin^2 \frac{z}{2} + 1]^{-1/2} = \sum_{n=1}^{\infty} a_n \sin^2(\frac{1}{2}nz); \quad \alpha = \frac{3}{8k_F^2 l^2} \quad (\text{A1})$$

For a low T expansion it is efficient to perform a duality transformation using the Poisson sum:

$$\sum_m g(m) = \int_{-\infty}^{\infty} d\phi \sum_p e^{2\pi i \phi p} g(\phi) \quad (\text{A2})$$

where the sums m, p run on all integers. Hence Eq. (1) becomes

$$\begin{aligned} Z &= Z_1 \int_{-\infty}^{\infty} d\phi \sum_p e^{2\pi i \phi(p + \phi_x) - \pi^2 t \phi^2} \times [1 - \\ &\alpha \sum_n a_n \int_0^\beta d\tau \int_0^\beta d\tau' \frac{\pi^2 T^2}{2 \sin^2[\pi T(\tau - \tau')]} (1 - \cos(2\pi n T \phi(\tau - \tau'))) \langle \cos[n(\theta(\tau) - \theta(\tau'))] \rangle_0] \end{aligned} \quad (\text{A3})$$

where $t = 2MR^2T$, $\beta = 1/T$, $Z_1 = \int \mathcal{D}\theta \exp(-S_1\{\theta\})$ and the $\langle \dots \rangle_0$ average is taken with respect to $\exp(-S_1)$, where

$$S_1\{\theta\} = \int_0^\beta d\tau \frac{1}{2} MR^2 \left(\frac{\partial \theta}{\partial \tau} \right)^2 \quad (\text{A4})$$

For a Gaussian average we have

$$\begin{aligned} \langle \cos[n(\theta(\tau) - \theta(\tau'))] \rangle_0 &= \exp[-\frac{1}{2}n^2 \langle (\theta(\tau) - \theta(\tau'))^2 \rangle_0] \\ &= \exp[-\frac{n^2}{\beta^2} \sum_\omega \langle |\theta(\omega)|^2 \rangle_0 (1 - \cos \omega(\tau - \tau'))] \\ &= \exp[-\frac{2n^2}{\beta^2 t} \sum_\omega \frac{1 - \cos \omega(\tau - \tau')}{\omega^2}] = e^{-n^2 |\tau - \tau'| / \beta t} \end{aligned} \quad (\text{A5})$$

where $\theta(\tau) = \frac{1}{\beta} \sum_\omega e^{-i\omega\tau} \theta(\omega)$ and ω are Matsubara frequencies $\omega = 2\pi T \times \text{integer}$.

For periodic functions we can change integration variables to $\tau_1 = \tau - \tau'$, $\tau_2 = \frac{1}{2}(\tau + \tau')$ with $\int d\tau_2 = \beta$, and $|\tau_1|$ in (A5) is chosen in the range $(-\beta/2, \beta/2)$ to allow for periodicity and continuity at $\tau_1 = 0$; hence,

$$\begin{aligned} Z &= Z_1 \int_{-\infty}^{\infty} d\phi \sum_p e^{2\pi i \phi(p + \phi_x) - \pi^2 t \phi^2} \times \\ &[1 - \beta\alpha \sum_n a_n \int_{-\beta/2}^{\beta/2} \frac{\pi^2 T^2}{2 \sin^2(\pi T \tau)} (1 - \cos(2\pi n T \phi \tau)) e^{-n^2 |\tau| / \beta t}] \end{aligned} \quad (\text{A6})$$

Integrating ϕ we obtain

$$\begin{aligned} Z \sim & \sum_p [e^{-\frac{(p + \phi_x)^2}{t}} - \beta\alpha \sum_n a_n \int_0^{\beta/2} \frac{\pi^2 T^2}{\sin^2(\pi T \tau)} (e^{-\frac{(p + \phi_x)^2}{t}} - \frac{1}{2} e^{-\frac{(p + \phi_x - nT\tau)^2}{t} - \frac{n^2 |\tau|}{\beta t}} \\ & - \frac{1}{2} e^{-\frac{(p + \phi_x + nT\tau)^2}{t} - \frac{n^2 |\tau|}{\beta t}})] \equiv \sum_p e^{-\frac{(p + \phi_x)^2}{t}} (1 - \frac{\delta F}{T}) \end{aligned} \quad (\text{A7})$$

where the correction to the free energy δF is

$$\begin{aligned} \delta F = \alpha \sum_p \frac{e^{-\frac{(p + \phi_x)^2}{t}}}{\sum_{p'} e^{-\frac{(p' + \phi_x)^2}{t}}} \sum_n a_n \int_0^{\beta/2} \frac{\pi^2 T^2}{\sin^2(\pi T \tau)} [& 1 - \frac{1}{2} e^{2n \frac{T}{t} \tau (p + \phi_x) - n^2 \frac{T^2}{t} \tau^2 - n^2 \frac{T}{t} \tau} \\ & - \frac{1}{2} e^{-2n \frac{T}{t} \tau (p + \phi_x) - n^2 \frac{T^2}{t} \tau^2 - n^2 \frac{T}{t} \tau}] \end{aligned} \quad (\text{A8})$$

where actually $\frac{T}{t} = 1/2MR^2$. At small τ there are $\int d\tau/\tau$ integrals and therefore a cutoff $1/\omega_c$ is needed. At low temperatures $t \ll 1$ one can retain only $p = p' = 0$ and then the cutoff is not needed, as found below. Hence for $t \ll 1$,

$$\delta F = \alpha \sum_n a_n \int_0^{\beta/2} \frac{\pi^2 T^2}{\sin^2(\pi T \tau)} [1 - e^{-n^2 \frac{T^2}{t} \tau^2 - n^2 \frac{T}{t} \tau} \cosh(2n\tau \phi_x T/t)] + O(e^{-1/t} \ln \omega_c T) \quad (\text{A9})$$

The effective mass M^* is defined in terms of the curvature, so that the 1st order correction is

$$\delta \frac{1}{M^* R^2} = \frac{\partial^2 \delta F}{\partial \phi_x^2} \Big|_0 = -\alpha \sum_n a_n \int_0^{\beta/2} \frac{\pi^2 T^2}{\sin^2(\pi T \tau)} (2n\tau T/t)^2 e^{-n^2 \frac{T^2}{t} \tau^2 - n^2 \frac{T}{t} \tau} \quad (\text{A10})$$

Note that there is no divergence at $\tau = 0$. The dominant integration range is $\tau < t/Tn^2$ so that the 1st term in the exponent can be expanded; keeping terms to order t^2 we obtain in terms of $x = \tau n^2 / 2MR^2$,

$$\begin{aligned} \delta \frac{M}{M^*} &= -2\alpha \sum_n a_n \int_0^\infty (1 + \frac{\pi^2 t^2}{3n^4} x^2 - \frac{t}{n^2} x^2 + \frac{t^2}{2n^4} x^4 + \dots) e^{-x} dx \\ &= -2\alpha \sum_n a_n (1 - \frac{2t}{n^2} + (\frac{2\pi^2}{3} + 12) \frac{t^2}{n^4} + \dots) \end{aligned} \quad (\text{A11})$$

Hence to 1st order in t

$$\frac{M}{M^*} = 1 - 2\alpha \sum_n a_n + 4t\alpha \sum_n \frac{a_n}{n^2} \quad (\text{A12})$$

At $t = 0$ this result is consistent with Eq. 9 of Ref. 13.

The following sum rules are useful for evaluating these sums. Integrating Eq. (A1) $\int_0^\pi dz$ we obtain:

$$\sum_{n=1}^{\infty} a_n = 2 - \frac{2}{\pi} \int_0^\pi \frac{dz}{\sqrt{4r^2 \sin^2 \frac{1}{2}z + 1}} \quad (\text{A13})$$

Fourier transform of Eq. (A1)

$$a_n = \frac{-4}{\pi} \int_0^\pi \left(1 - \frac{1}{\sqrt{4r^2 \sin^2 \frac{1}{2}z + 1}} \right) \cos nz \, dz \quad (\text{A14})$$

and performing the n summation, we obtain

$$\sum_{n=1}^{\infty} \frac{a_n}{n^2} = \frac{4}{\pi} \int_0^\pi \frac{1}{\sqrt{4r^2 \sin^2 \frac{1}{2}z + 1}} \left(\frac{\pi^2}{6} - \frac{\pi z}{2} + \frac{z^2}{4} \right) dz. \quad (\text{A15})$$

ACKNOWLEDGMENTS

We thank C. Herrero for valuable help with the numerical code. We also appreciate useful discussions with A. Aharony, A. Altshuler, D. Cohen, Y. Gefen, A. Golub, D. Golubev, I. Gornyi, F. Guinea, Y. Imry, A. Mirlin, D. Polyakov and A. D. Zaikin. This research was supported by the Deutsch-Israelische Projektkooperation (DIP) and by THE ISRAEL SCIENCE FOUNDATION founded by the Israel Academy of Sciences and Humanities.

-
- ¹ R. A. Webb, S. Washburn, C. P. Umbach, and R. B. Laibowitz, Phys. Rev. Lett. **54**, 2696 (1985).
² E. M. Q. Jariwala, P. Mohanty, M. B. Ketchen, and R. A. Webb, Phys. Rev. Lett. **86**, 001594 (2001).
³ K. Yu. Arutyunov and T. T. Hongisto, Phys. Rev. B **70**, 064514 (2004).
⁴ I. Neder, M. Heiblum, Y. Levinson, D. Mahalu, and V. Umansky, Phys. Rev. Lett. **96**, 016804 (2006).
⁵ D. M. Harber, J. M. McGuirk, J. M. Obrecht and E. A. Cornell, J. Low Temp. Phys. **133**, 229 (2003).
⁶ M. P. A. Jones, C. J. Vale, D. Sahagun, B. V. Hall and E. A. Hinds, Phys. Rev. Lett. **91**, 080401 (2003).
⁷ Y. J. Lin, I. Teper, C. Chin and V. Vuletić, Phys. Rev. Lett. **92**, 050404 (2004).
⁸ P. Hyafil, J. Mozley, A. Perrin, J. TAILLEUR, G. Noguez, M. Brune, J.M. Raimond, and S. Haroche, Phys. Rev. Lett. **93**, 103001 (2004).
⁹ F. Guinea, Phys. Rev. B **65**, 205317 (2002).
¹⁰ W. Hofstetter and W. Zwerger, Phys. Rev. Lett. **78**, 3737 (1997).
¹¹ C. P. Herrero, G. Schön and A. D. Zaikin, Phys. Rev. B **59**, 5728 (1999).
¹² M. Büttiker and A. N. Jordan, Physica E (Amsterdam) **29**, 272 (2005).
¹³ D. S. Golubev, C. P. Herrero and A. D. Zaikin, Europhys. Lett. **63**, 426 (2003).
¹⁴ B. Horovitz and P. Le Doussal, Phys. Rev. B **74**, 073104 (2006).
¹⁵ The RG results of [9] are in fact consistent with $\mu = 0$ [F. Guinea, private communication].
¹⁶ B. Horovitz and D. Cohen, Europhys. Lett. **81**, 30001 (2008); D. Cohen and B. Horovitz J. Phys. A: Math. Theor. **40**, 12281 (2007).
¹⁷ A Guide to Monte Carlo simulations in Statistical Physics, D. P. Landau and K. Binder, Cambridge University Press (2000)